

# Low Temperature Ethanol Sensors using Cerium doped Tin oxide Nanostructures

Anima Johari\* and M.C.Bhatnagar

Physics Department, IIT Delhi, Hauz Khas New Delhi 110016 INDIA

\* CARE , IIT Delhi, Hauz Khas New Delhi 110016 INDIA

## Abstract:

Volatile organic compound (VOC) vapors are the primary sources of environmental pollutants in houses and workplaces and there is need to develop low temperature, sensitive and selective gas sensors to monitor the gas content. In this paper, we have discussed the effect of cerium (Ce) doping in SnO<sub>2</sub> nanostructures on the structural and gas sensing properties. The nanostructures have been synthesized by thermal evaporation process. The structural and surface morphology studies confirm the growth of nanowires on silicon substrates. High resolution transmission electron microscopy analysis confirms the growth of uniform and well crystallized nanowires. The corresponding EDX spectra also confirm the doping of Ce into SnO<sub>2</sub> nanowires. The gas sensor response of Ce-doped SnO<sub>2</sub> nanowires was investigated upon exposure to ethanol and other gases. It was observed that doping of Ce enhances the ethanol sensitivity of nanowire based sensors at low temperature and the sensor response improves with increase in ethanol concentration.

**Keywords:** CeO<sub>2</sub> doped SnO<sub>2</sub> nanostructures, ethanol sensor, low temperature sensor

## Introduction :

These days, Volatile organic compound (VOC) vapors are the primary sources of environmental pollutants in houses and workplaces and are therefore considered harmful to the human body [1,2,3]. So far a number of sensors have been developed using SnO<sub>2</sub> [6,7] WO<sub>3</sub> [8], ZnO [9], and TiO<sub>2</sub> [10] to monitor VOC gases. SnO<sub>2</sub> nanostructure based sensors have been reported to show good sensitivity properties such as low detection limit, good selectivity, and short response and recovery time [22].

The modification of structure and grain size or introducing an impurity level and surface defects in tin oxide through doping is an effective way to improve its gas sensing properties. Cerium as a dopant has received great attention due to its peculiar properties arising from the availability of the 4f shell. Upto now, some reports are available on gas sensing applications of Ce-doped SnO<sub>2</sub>. For example, Jiang et al. [28] prepared highly sensitive and selective butanone sensors based on Ce-doped SnO<sub>2</sub> thin film. Ce-doped SnO<sub>2</sub> nanomaterials have been used to improve ethanol response selectivity in presence of CO, LPG and CH<sub>4</sub> [29]. Ce-doped nanoparticles have been used for detection of ethanol [30].

The present study aims to synthesize Ce-doped SnO<sub>2</sub> powder and successive growth of Ce-doped SnO<sub>2</sub> nanostructures by thermal evaporation of powder. The effect of Ce doping concentrations on the surface, structural and gas sensing properties of the processed powder and nanostructures is also studied.

## Experimental details

The synthesis of Ce-doped SnO<sub>2</sub> nanostructures involves two step processes. Firstly, Ce-doped SnO<sub>2</sub> powder was prepared by sol gel process. In this process, SnCl<sub>4</sub>.5H<sub>2</sub>O and Ce(NO<sub>3</sub>)<sub>3</sub>.6H<sub>2</sub>O were used as precursors. Finally, Ce-doped SnO<sub>2</sub> powder with different mass ratio was formed. Sequentially, Ce-doped SnO<sub>2</sub> nanowires were synthesized by thermal evaporation process. In this process, as synthesized Ce-doped SnO<sub>2</sub> powder was used as source powder and silicon substrate (Si) were loaded in horizontal tubular furnace in a way that source powder was placed in maximum temperature zone and Si substrate was placed at some distance from the source powder. The furnace was then allowed to heat from room temperature to 1050 °C in nitrogen ambience (1000 sccm) and substrate temperature was maintained at 700 °C. The process temperature was maintained at 1050°C for 1 hour and then cooled to room

temperature. The growth of nanostructures occurs on Si substrate due to thermal evaporation and condensation of source powder.

For as-synthesized samples, morphological investigations were performed using Scanning electron microscopy (SEM, ZEISS EVO-50) equipped with energy dispersive X-ray spectroscopy (EDX, RONTEC) and transmission electron microscope (TEM, Philips CM12). The crystallographic interpretations were performed by X-ray diffractometer (XRD, Philips X'pert Pro diffractometer) and high resolution transmission electron microscopy image (HRTEM, Philips CM-200 microscope). To investigate the gas sensing characteristics of as-synthesized Ce-doped  $\text{SnO}_2$ , two types of sensors were fabricated. Ce-doped  $\text{SnO}_2$  nanowires based sensor was fabricated by placing a drop of dilute suspension of nanowires on  $\text{SiO}_2$ /silicon substrate. This substrate has pre-fabricated gold electrodes. All of the sensors were tested in lab made set up.

### Results and Discussion:

Figure 1(a) and (b) shows the SEM images of nanowires grown on Si substrates using source precursor with mass ratio of 0.05 and 0.1 respectively. The wire like morphology of as-synthesized Ce-doped  $\text{SnO}_2$  nanostructures with lengths of about 40-60  $\mu\text{m}$  and diameter of few tens of nanometers was also confirmed. The magnified SEM images (inset of (a) and (b)) shows the

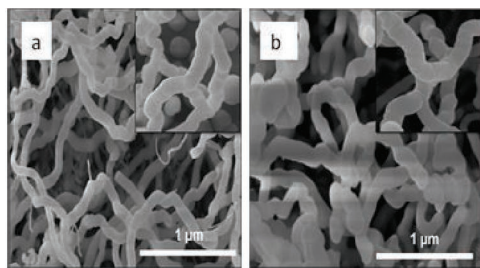


Fig. 1. SEM images of nanowires grown on Si substrate with  $\text{CeO}_2:\text{SnO}_2$  mass ratio of 0.05 (a) and 0.1 (b). Inset shows high magnification images.

rough surfaces and repetitive arrangement of a particular pattern in as-synthesized nanowires, these rough surfaces may be due to Ce incorporation into  $\text{SnO}_2$  nanowires.

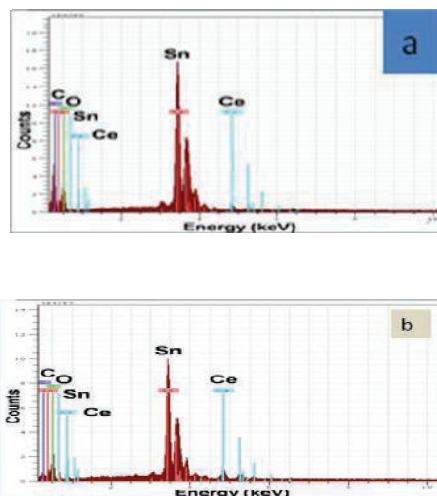


Fig. 2. EDX spectrum, showing the chemical composition of the Ce-doped  $\text{SnO}_2$  nanowires produced using source precursor of with  $\text{CeO}_2:\text{SnO}_2$  mass ratio of 0.05 (a) and 0.1 (b).

Figure 2 shows the EDX spectrum corresponding to  $\text{CeO}_2:\text{SnO}_2$  mass ratio of 0.05 and 0.1 annealed at 1050  $^{\circ}\text{C}$  of as-synthesized nanowires ((a) and (b)). The EDX patterns reveal that tin, oxygen and cerium are the only components present. No contamination was found in the product. Carbon peak is present due to coating, which was deposited during sample preparation. From the quantitative EDX analysis, the Ce-doping concentration into as-grown  $\text{SnO}_2$  nanowires was found to be 0.2 at% (a) to 1 at% (b), corresponding to 5 at% and 10 at% of Ce-doped  $\text{SnO}_2$  powder.

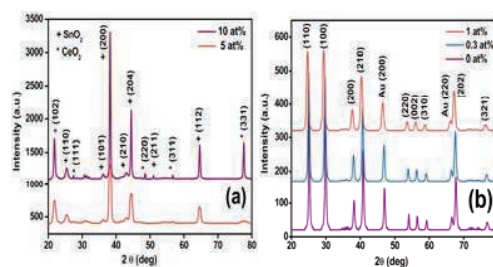


Fig.3. X-ray diffraction patterns of (a) Ce-doped  $\text{SnO}_2$  nanoparticles and (b) undoped and Ce-doped  $\text{SnO}_2$  nanowires

Figure 3 (a) showed X-ray diffraction patterns of Ce-doped  $\text{SnO}_2$  nanoparticles with Ce concentration of 5 at% and 10 at%. From these patterns, it was observed that the strong diffraction peaks of the  $\text{SnO}_2$  with tetragonal rutile structure (JCPDS No. 41-

1445) became sharper with the increasing amount of Ce, which indicated doping Ce can improve the crystallization of the SnO<sub>2</sub>. It is also speculated that the doping of Ce has changed the crystallite size of SnO<sub>2</sub> and these result indicates the particle size of the doped SnO<sub>2</sub> is larger than that of the undoped SnO<sub>2</sub>. For Ce content of 10 at%, the cubic structure of CeO<sub>2</sub> (JCPDS No. 81-0792) was appeared however for Ce concentration of 5 at%, no peaks corresponding to CeO<sub>2</sub> exists. Figure 3 (b) showed X-ray diffraction patterns of Ce-doped SnO<sub>2</sub> nanowires with different Ce concentrations of 0.3 at% and 1 at%. In this pattern, the tetragonal rutile phase of SnO<sub>2</sub> (JCPDS No. 41-1445) is detected with no clear evidence of impurities, regardless of dopant concentration and no peak corresponding to CeO<sub>2</sub> is visible.

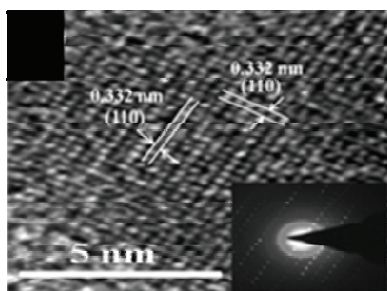


Fig. 4. Bright field (BF) transmission electron microscopy (TEM) images of Ce doped SnO<sub>2</sub> nanowires with concentration of 5 at%

Figure 4 (e) shows the high resolution TEM image and SAED pattern of Ce-doped SnO<sub>2</sub> nanowire with Ce concentration of 1 at%. This image concludes that this particular wire is a structurally uniform single crystal. The measured interplanar spacing of the lattice fringes of selected nanowire is about 0.332 nm, corresponding to the distance of the neighboring (110) planes in tetragonal rutile SnO<sub>2</sub> structure. The SAED pattern in the inset also indicated a single crystallinity of Ce-doped SnO<sub>2</sub> nanowires having a rutile structure with processed the growth direction aligned along the (110) direction. These are in agreement with the standard data (JCPDS: 41-1445).

To investigate the gas sensing properties of Ce-doped SnO<sub>2</sub> nanowires. Fig. 5 shows the single nanowire sensor assembly.

Ce doped sensors with single (A) and multiple (B) nanowires were tested at different temperatures ranging from 50 to 400 °C with an interval of 50 °C to optimize working temperature exposed to different gases.

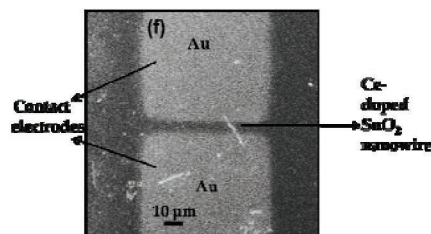
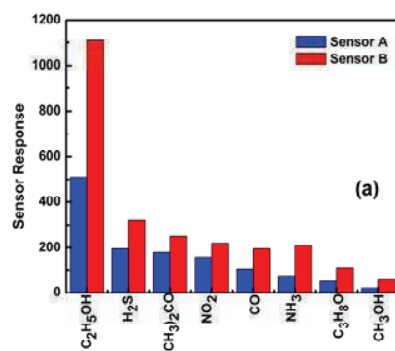


Fig. 5 Single nanowire assembly

The response of sensor A and B, when exposed at the same time with various selected reducing and oxidizing gases are illustrated in figure 6(a), were found to be highly sensitive and selective to ethanol as compared to other exposing gases. The comparative ethanol response of sensor A and B measured at a temperature of 200 °C for ethanol concentrations of 50 ppm are illustrated in figure 6 (b) and concludes that the sensitivity, response time and recovery time of sensor B has been modified as compared to sensor A. On increasing ethanol concentration in air from 50 ppm to 500 ppm, the surface reaction increases due to a large surface coverage of ethanol molecules, resulting in higher response (figure 6c). The linear sensor response was observed from the response of sensor A and B at the operating temperature of 200 °C for different concentrations of ethanol. The variation of sensor response with measurement temperature, as illustrated in figure 6 (d), confirms that the response of both types of sensors (A and B) was enhanced rapidly at optimized measurement temperature of 200 °C.



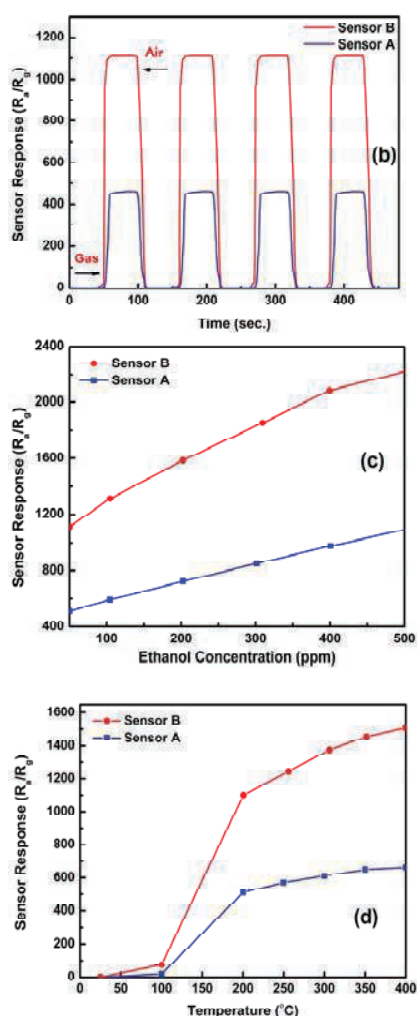


Fig. 6 Sensor responses of Sensor A and B (a) sensor response curve measured at 200 °C for 50 ppm of various gases (b) response curve for ethanol (50 ppm) (c) Variation of sensor response with ethanol concentration (d) sensor response as a function of operating temperature for ethanol concentration of 50 ppm.

## Conclusions

In summary, we have synthesized Ce-doped SnO<sub>2</sub> powder by sol-gel method and successively nanowires were grown on Si substrate by thermal evaporation of as-synthesized powder. The surface morphology study confirms the growth of nanowires on Si substrate. The nanowires have tetragonal rutile structure of SnO<sub>2</sub>. The cubic structure of CeO<sub>2</sub> is also detected in nanoparticles. The corresponding EDX spectra confirm the doping

of Ce into SnO<sub>2</sub> lattice with Ce concentration of 5-10 at% and 0.3-1 at% in nanoparticles and nanowires respectively. The gas sensor response of Ce-doped SnO<sub>2</sub> nanowires was studied upon exposure to different gases. It was observed that doping of Ce enhances the ethanol sensitivity of nanowire based sensors and the sensor response improves with increase in ethanol concentration. However Ce-doped SnO<sub>2</sub> nanowires are more sensitive for ethanol at lower temperatures compared to nanoparticles. This sensing behaviour offers a suitable application of the Ce-doped SnO<sub>2</sub> nanowire sensor for detection of ethanol gas.

## References:

- [1] Franciosa L, Forleoa A, Taurino A, et al., Sens Actuators 2008; B134: 660-5.
- [2] Sanchez Jean-Baptiste, Berger Franck, Fromm Michel, Nadal Marie-Helene, Sens Actuators 2006; B119: 227-33.
- [3] Rella R, Spadavecchia J, Manera MG, Capone S, Taurino A, Martino M, et al., Sens and actuators 2007; B127: 426-31.
- [4] D.S. Lee, J.K. Jung, J.W. Lim, J.S. Huh, D.D. Lee, Sens. Actuators B: Chem. 77 (2001) 228–236.
- [5] W. Zeng, T.M. Liu, Z.C. Wang, Journal of Materials Chemistry 22 (2012) 3544–3548.
- [6] K. Kanda, T. Maekawa, Sens. Actuators B: Chem. 108 (2005) 97–101.
- [7] N.H. Al-Hardan, M.J. Abdullah, A. Abdul Aziz, H. Ahmad, L.Y. Low, Vacuum 85 (2010) 101–106.
- [8] A.M. Taurino, S. Capone, P. Siciliano et al., Sens. Actuators B: Chem. 92 (2003) 292–302.
- [9] Wang C, Chu X F and Wu M M, Sens. and Actuators B 120 508–13.
- [10] Z.W. Jiang, Z. Guo, B. Sun, Y. Jia, M.Q. Li, J.H. Liu, Sens. and Act. B: Chemical 145 (2010) 667–673.
- [11] F. Pourfayaz, A. Khodadadi, Y. Mortazavi, S.S. Mohajerzadeh, Sens. Actuators B 108 (2005) 172–176.

- [12] Dejun Liu, Tianmo Liu, Hejing Zhang, et.al., Materials Science in Semiconductor Processing 15 (2012) 438–444.